Angle-dependent decoherence of charge qubits in free-standing slabs

2010 J. Phys.: Condens. Matter 22 045301

(http://iopscience.iop.org/0953-8984/22/4/045301)

IOP PUBLISHING JOURNAL OF PHYSICS: CONDENSED MATTER

J. Phys.: Condens. Matter **22** (2010) 045301 (6pp) doi:10.1088/0953-8984/22/4/045301

Angle-dependent decoherence of charge qubits in free-standing slabs

Ying-Yen Liao[1], Yueh-Nan Chen[2] and Sheng-Rui Jian[3]

[1] Department of Applied Physics, National University of Kaohsiung, Kaohsiung 811, Taiwan
[2] Department of Physics and National Center for Theoretical Sciences, National Cheng-Kung University, Tainan 701, Taiwan
[3] Department of Materials Science and Engineering, I-Shou University, Kaohsiung 840, Taiwan

E-mail: yyliao@nuk.edu.tw

Received 21 June 2009, in final form 18 November 2009
Published 5 January 2010
Online at stacks.iop.org/JPhysCM/22/045301

Abstract
We investigate the decoherence of a charge qubit in a double quantum dot which is formed in a free-standing semiconductor slab. The dots are spatially arranged to align along a particular direction. Confined phonons in the slab have a remarkable influence on the dynamics of a qubit system. We show that the decoherence of such a qubit strongly depends on the positions of the dots. By varying the tunnel coupling, the decoherence differs significantly in laterally and vertically coupled quantum dots. A robust qubit is further achieved due to suppression of electron–phonon coupling. Moreover, the coherent evolution of the system is analyzed by modulating the interdot direction.

1. Introduction

Understanding and controlling the behavior of electrons in nanostructures leads to an entirely new class of devices, such as the sensors and electronics ranging from photon detectors to quantum computers [1–4]. Nanostructured devices possess a significant advantage of direct controllability with the help of external voltages [5, 6]. For quantum computation, a double quantum dot is proposed to realize a functional quantum bit (qubit). Correspondingly, a two-level quantum system is established by employing charge degrees of freedom [7–9]. The locations of the electron in the dots subsequently represent two logical states of the qubit. In such a device, quantum superpositions in double quantum dots can be coherently controlled in terms of the charge states [7–9].

Since semiconductor quantum dots are solid-state structures, the operations of qubits are strongly limited by the decoherence which is induced by couplings to the environment. The electron–phonon interaction is one of the major sources of decoherence [10–13]. In the context of qubit realization, some functions of double dot qubits have been demonstrated in recent experiments [7–9]. Extensive theoretical works are devoted to single [14–18] and coupled qubits [19, 20] which are perturbed by bulk baths. In this work, we aim to search for ways to extend the decoherence time if the quantum dots are placed in a specific environment. For a charge qubit, it is expected that the decoherence time is extended by means of reducing the electron–phonon coupling. With the advance of nanotechnology, the ability to design geometries opens up a number of interesting possibilities, i.e. the electron–phonon coupling can be engineered at the origin. Unlike bulk cases, the engineered structure supports the tailoring effect of the phonon density of states by altering the dimensions [21–25]. Therefore, a charge qubit in the engineered structure is expected to reveal interesting properties.

In this paper, we investigate the decoherence of a double dot qubit which is embedded in a free-standing semiconductor slab. An electron in this qubit interacts with the confined phonons in the slab. The dots are oriented along a particular direction with respect to the surface of the slab. Then the dominant decoherence contributor can be tuned by orienting the dot structure. With the master equation, we analyze the dynamics of the qubit in the Born–Markov approximation. A high-quality qubit is obtained by varying the tunnel detuning. Two distinct tendencies are exhibited in the laterally and vertically coupled dots. It is observed that the decoherence of a qubit strongly depends on the interdot orientation. Furthermore, in the slab system, inhibition of the electron–phonon coupling can be achieved, leading to a robust qubit.

2. Model and method

A scheme of our model is depicted in figure 1. A qubit consists of two coupled quantum dots embedded in a free-standing semiconductor slab. Most of the structure is spatially separated from most of the substrate [26, 27]. The in-plane scale of the slab is assumed to substantially exceed the width w and the dot size a. This assumption ensures that the effect of the contacts with the substrate can be neglected in the system. The quantum dots are spatially oriented along a certain direction. The interdot distance and angle are d and Φ, respectively. We assume that only one additional electron is allowed to exist on either the left or the right dot in the Coulomb blockade regime. The effective Hilbert space of the electronic system can be defined by the basis states: $|L\rangle$ for one excess electron in the left dot and $|R\rangle$ for one excess electron in the right dot [10]. To study the decoherence of a free-standing qubit, the total Hamiltonian can then be expressed as

$$H = H_{\mathrm{e}} + H_{\mathrm{p}} + H_{\mathrm{ep}}, \tag{1}$$

with

$$H_{\mathrm{e}} = \frac{\varepsilon}{2}\sigma_z + T_{\mathrm{c}}\sigma_x, \tag{2}$$

$$H_{\mathrm{p}} = \sum_{\mathbf{q}_\parallel} \hbar\omega_{\mathbf{q}_\parallel} b^{\dagger}_{\mathbf{q}_\parallel} b_{\mathbf{q}_\parallel}, \tag{3}$$

$$H_{\mathrm{ep}} = \frac{\sigma_z}{2} \sum_{\mathbf{q}_\parallel} M_{\mathbf{q}_\parallel} (b^{\dagger}_{\mathbf{q}_\parallel} + b_{-\mathbf{q}_\parallel}), \tag{4}$$

where H_{e} is the electron Hamiltonian, H_{p} is the phonon bath and H_{ep} is the electron–phonon interaction in the slab. The Pauli matrices σ_x and σ_z denote $|L\rangle\langle R| + |R\rangle\langle L|$ and $|L\rangle\langle L| - |R\rangle\langle R|$, respectively. ε is the electron energy difference and T_{c} is the tunnel coupling between the charge states $|L\rangle$ and $|R\rangle$. In experiments, the parameters ε and T_{c} can be controlled through the external gate voltages [7–9]. $\omega_{\mathbf{q}_\parallel}$ and $b^{\dagger}_{\mathbf{q}_\parallel}$ ($b_{\mathbf{q}_\parallel}$) are the frequency and creation (annihilation) operator of the phonons with the in-plane wavevector $\mathbf{q}_\parallel$. In addition, $M_{\mathbf{q}_\parallel}$ denotes the coupling element of electrons to phonons in the slab. Note that, in our model, T_{c} is assumed to be nonzero so that the electron is allowed to tunnel back and forth between two dots. During the evolution of the qubit, the populations of the states will be damped with time, leading to a relaxation dynamics, i.e. we do not consider the pure dephasing case.

For confined phonons, the dispersion relation can be derived from the elastic continuum model [28]. Different phonon modes in the slab are subsequently defined by applying the second quantization formalism [29, 30]. One can obtain the phonon frequency through numerical treatment. There are infinitely many branches for each in-plane component $q_\parallel$. For the free-standing slab, the importance of the piezoelectric potential and deformation potential is obviously different from that for bulk systems [10, 11]. The ratio of the piezoelectric potential strength to the deformation potential strength is equal to $(ee_{14}/E_a q)^2$, where e denotes the electron charge, e_{14} is the piezoelectric constant, E_a is the deformation potential constant, and q is the phonon wavevector. For long-wavelength phonons, the piezoelectric interaction is the dominant term in bulk systems. For a slab, however, a lower bound

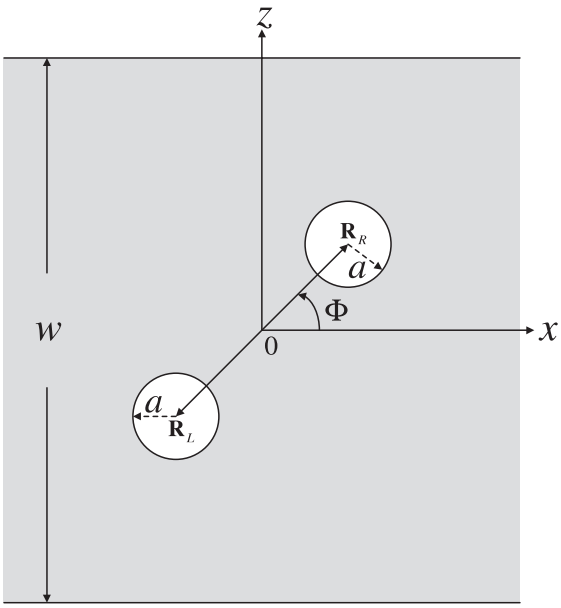

Figure 1. Schematic illustration of a double dot qubit embedded in a free-standing slab with a width w. The radius of the dots is a and the surfaces of the slab are $z = \pm w/2$. The dots are arranged to orient in a particular direction, corresponding to an angle Φ with respect to the x direction. The position vectors of the left and the right dots are $\mathbf{R}_L = -\mathbf{d}/2$ and $\mathbf{R}_R = \mathbf{d}/2$, respectively.

for the wavelength is obtained due to the confinement in geometry. This fact cuts off small phonon momenta that determine the strength of the piezoelectric coupling. Based on this argument, the deformation potential prevails over the piezoelectric potential in the slab system [30–32]. To explain the main feature of our model, the deformation potential is supposed to be the main contributor. Consequently, there are two relevant acoustic modes: dilatational waves and flexural waves. On the contrary, shear waves are neglected because of their vanishing interaction with the electron [30]. The dispersion relation for the dilatational waves is described by

$$\omega_{\mathbf{q}_\parallel} = c_l\sqrt{q_\parallel^2 + q_l^2} = c_t\sqrt{q_\parallel^2 + q_t^2}, \tag{5}$$

where the parameters q_l and q_t can be determined from the equation [30]

$$\frac{\tan q_t d/2}{\tan q_l d/2} = -\frac{4q_\parallel^2 q_l q_t}{(q_\parallel^2 - q_t^2)^2}. \tag{6}$$

Similarly, for the flexural waves, one can obtain the parameters q_l and q_t by solving the equation [30]

$$\frac{\tan q_l d/2}{\tan q_t d/2} = -\frac{4q_\parallel^2 q_l q_t}{(q_\parallel^2 - q_t^2)^2}, \tag{7}$$

together with the dispersion relation (equation (5)). For two waves, the parameters $q_\parallel$, q_l and q_t independently satisfy the dispersion relations. Next, we investigate the effect of a phonon bath on an electron existing in a double quantum dot system. An isotropic electron wavefunction is assumed to be sharply dispersed around the center of

quantum dot with a Gaussian shape. From the positions of the dots, the wavefunctions for the two states are $\psi_{L(R)}(\mathbf{r}) = \exp[-|\mathbf{r} - \mathbf{R}_{L(R)}|^2/2a^2]/\sqrt{\pi^{3/2}a^3}$, where $\mathbf{r} = (x, y, z)$, $\mathbf{R}_L = [-d\cos(\Phi)/2, 0, -d\sin(\Phi)/2]$ and $\mathbf{R}_R = [d\cos(\Phi)/2, 0, d\sin(\Phi)/2]$. As shown in figure 1, the position of the dot plays a crucial role in the electron–phonon interaction. For dilatational waves, the coupling element is formulated by

$$M_{\mathbf{q}_\parallel} = \lambda_{\mathrm{d}} \mathrm{e}^{-(q_\parallel^2+q_l^2)a^2/4}\left(\mathrm{e}^{\mathrm{i}\mathbf{q}_\parallel\cdot\mathbf{d}/2} - \mathrm{e}^{-\mathrm{i}\mathbf{q}_\parallel\cdot\mathbf{d}/2}\right), \tag{8}$$

where the coupling strength is

$$\lambda_{\mathrm{d}} = F_{\mathrm{d}}\sqrt{\frac{\hbar E_a^2}{2A\rho\omega_{\mathbf{q}_\parallel}}}(q_t^2 - q_\parallel^2)(q_l^2 + q_\parallel^2)\sin(q_t w/2) \times \cos\left[q_l d\sin(\Phi)/2\right]. \tag{9}$$

In contrast, for flexural waves, the coupling element is formulated by

$$M_{\mathbf{q}_\parallel} = -\lambda_{\mathrm{f}} \mathrm{e}^{-(q_\parallel^2+q_l^2)a^2/4}\left(\mathrm{e}^{\mathrm{i}\mathbf{q}_\parallel\cdot\mathbf{d}/2} + \mathrm{e}^{-\mathrm{i}\mathbf{q}_\parallel\cdot\mathbf{d}/2}\right), \tag{10}$$

with its strength

$$\lambda_{\mathrm{f}} = F_{\mathrm{f}}\sqrt{\frac{\hbar E_a^2}{2A\rho\omega_{\mathbf{q}_\parallel}}}(q_t^2 - q_\parallel^2)(q_l^2 + q_\parallel^2)\cos(q_t w/2) \times \sin\left[q_l d\sin(\Phi)/2\right]. \tag{11}$$

Here, A is the area of the slab, ρ is the mass density, and F_{d} (F_{f}) is the normalization constant of the dilatational (flexural) waves.

A master equation for the system dynamics is now derived in the standard way [33–35]. The Born–Markov approximation is performed in our model. In addition, the system and the phonon bath are assumed to be disentangled at $t = 0$. Then, the master equation for the density matrix $\rho(t)$ can be written as

$$\frac{\mathrm{d}\rho(t)}{\mathrm{d}t} = -\frac{\mathrm{i}}{\hbar}[H_{\mathrm{e}}, \rho(t)] - \frac{1}{\hbar^2}\int_0^\infty \mathrm{d}t'[S, \tilde{S}(t'-t)\rho(t)] \times K(t-t') + \frac{1}{\hbar^2}\int_0^\infty \mathrm{d}t'[S, \rho(t)\tilde{S}(t'-t)]K(t'-t). \tag{12}$$

Here, $\tilde{S}$ is the interaction picture of the operator $S = \sigma_z/2$ and the bath correlation function is

$$K(\tau) = \int_0^\infty \mathrm{d}\omega J(\omega)[\cos(\omega\tau)\coth(\hbar\omega/2k_{\mathrm{B}}T) - \mathrm{i}\sin(\omega\tau)], \tag{13}$$

with the Boltzmann constant k_{B}, temperature T, and spectral density J which is given by

$$J(\omega) = \sum_{\mathbf{q}_\parallel} |M_{\mathbf{q}_\parallel}|^2 \delta(\omega - \omega_{\mathbf{q}_\parallel}). \tag{14}$$

In equation (14) the function contains all relevant information about the environment and the coupling to the electron. It is worth mentioning that low temperature and the one-phonon process are considered in our calculations. When the temperature is high, the two-phonon process is important [36]. However, the effect of the two-phonon process becomes much weaker than that of the one-phonon process at low temperature. Accordingly, the higher order processes are neglected in the model.

We now study the specific case that the electron is initially prepared in the left dot. When the tunnel coupling is driven, the electron can resonantly tunnel back and forth between two dots. According to these conditions ($n_L(t = 0) = 1$ and $\varepsilon = 0$), one can follow the standard treatment [33–35] to obtain the population of the left-dot state

$$n_L(t) \simeq \tfrac{1}{2}[1 + \mathrm{e}^{-t/T_{\mathrm{d}}}\cos(\omega t)], \tag{15}$$

where n_L denotes the expectation value $\langle L|\rho(t)|L\rangle$, the oscillation frequency is

$$\omega \simeq \frac{2T_{\mathrm{c}}}{\hbar}, \tag{16}$$

and the decoherence time is

$$T_{\mathrm{d}} = \frac{4\hbar^2}{\pi J(2T_{\mathrm{c}}/\hbar)\coth(T_{\mathrm{c}}/k_{\mathrm{B}}T)}. \tag{17}$$

Moreover, the population of the right-dot state n_R is simply estimated by $1 - n_L$. From equation (15), one realizes that two parameters govern the operation of the qubit. It is evidently shown that the tunnel coupling determines the oscillation of the evolution. However, the time-dependent population will be damped by the decoherence time. Based on two scales, thus, the quality factor is defined as [16–18]

$$Q = \frac{\omega T_{\mathrm{d}}}{2\pi}, \tag{18}$$

which quantifies the stability of the quantum system under the action of the electron–phonon interaction. In the calculations, we set $a = 25$ nm, $d = 50$ nm, $w = 120$ nm, and $T = 50$ mK. The parameters for GaAs material are $\rho = 5.3 \times 10^3$ Kg m^{-3}, $E_a = 2.2 \times 10^{-18}$ J, $c_t = 3.0 \times 10^3$ m s^{-1}, and $c_l = 5.2 \times 10^3$ m s^{-1} [37].

3. Results and discussion

Figure 2 presents the tunnel coupling dependence of the quality factor of a qubit prepared in the case of $\Phi = 0$, i.e. the dots align along the x direction. The flexural waves do not contribute any effect to the decoherence. One can find a high-quality factor in the small T_{c} regime. The curve decreases to a minimum with increasing tunnel coupling. Variation of the quality factor by up to several orders of magnitude can be tuned in such a system, because of the influence of spectral density shown in the inset of Figure 2. For small T_{c}, the spectral density is relatively small, leading to a long decoherence time T_{d}. The weak phonon influence directly enhances the quality factor. Moreover, a remarkable quality factor ($Q \to \infty$) is found by appropriately varying the tunnel coupling ($T_{\mathrm{c}} \approx 36.55$ μeV). This explicitly indicates that the quantum coherence stays in the free-standing qubit for a long time. As shown in the inset, the long coherence results from a drastic suppression of J ($\to 0$) at the value of 73.1 μeV, corresponding to the ineffective electron–phonon interaction [31, 32]. In a real

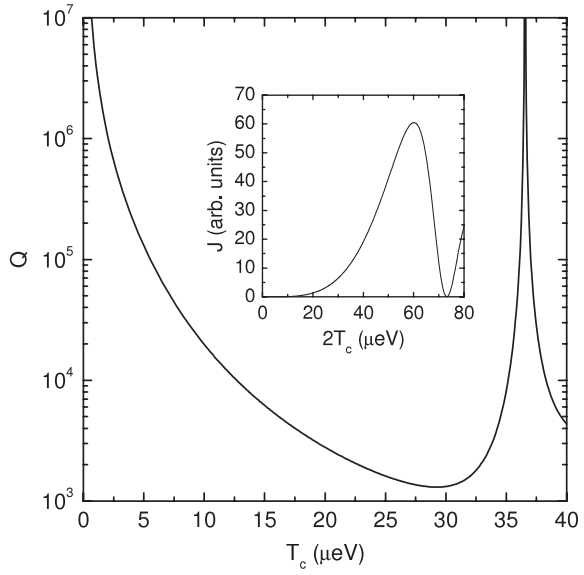

Figure 2. Quality factor Q as a function of tunnel coupling T_c for $\Phi = 0$. The inset shows the spectral density of the dilatational waves.

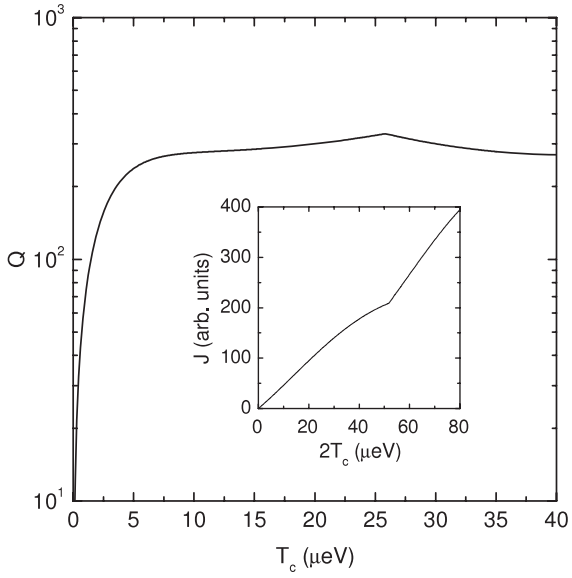

Figure 3. Quality factor Q as a function of tunnel coupling T_c for $\Phi = \pi/2$. The inset shows the spectral density of the flexural waves.

system, a slab has finite extension. Thus, the electron–phonon interaction cannot be completely suppressed. We expected that the singular behavior in quality factor would be smeared out, but the enhanced feature is still held.

A contrary case is shown in figure 3. Two quantum dots are assumed to be vertically coupled in the system ($\Phi = \pi/2$). The flexural wave becomes the main contributor due to $\mathbf{q}_\parallel \cdot \mathbf{d} = 0$. The quality factor presents a diverse behavior. When the tunnel coupling decreases, the value simultaneously decreases in the small T_c regime. This tendency differs from the case of $\Phi = 0$. From the inset diagram, the spectral density of flexural waves is high and varies more rapidly with respect to the tunnel coupling. A fast changing rate of the spectral density results in the fact that decoherence time becomes dominant over the oscillation. Furthermore, a cusp is found with the tunnel coupling. This result reflects that a new additional subband starts contributing an effect to the spectral density shown in the inset [31, 32]. We further contrast the magnitudes of quality factors in two different configurations. Actually, the value is lower in the vertically coupled system. As shown in the insets of figures 2 and 3, we compare the two numerical results to find that the spectral density of flexural waves is higher than that of dilatational waves and further analyze the contributing components in detail. For phonon properties, the flexural waves have a higher density of states at small $q_\parallel$ [38]. Moreover, the strength of the coupling element $|M_{\mathbf{q}_\parallel}|^2$ for $\Phi = \pi/2$ can be relatively enhanced due to $|e^{i\mathbf{q}_\parallel \cdot \mathbf{d}/2} - e^{-i\mathbf{q}_\parallel \cdot \mathbf{d}/2}|^2 = 4$. The arrangement of the dots also plays an important role in the spectral density of flexural waves.

To understand the effect of the spatial arrangement of quantum dots, in figure 4 we plot the angle-dependent quality factor for fixing $T_c = 20$ μeV. The quality factor gradually decreases with increasing angle Φ. We analyze the contribution of decoherence in this confined structure. When the interdot direction is oriented, the total contribution

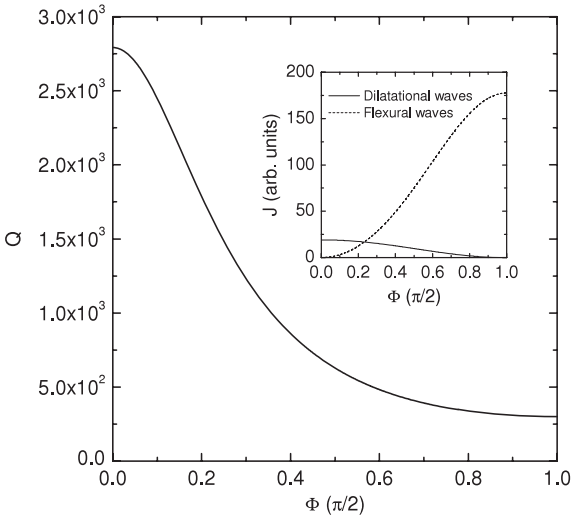

Figure 4. Angle dependence of the quality factor for $T_c = 20$ μ eV. Inset: spectral density of the dilatational and flexural waves.

consists of two components: dilatational waves and flexural waves. Both components contribute to the spectral density to different degrees, strongly depending on the corresponding angle shown in the inset. For small Φ, the dilatational waves govern the decoherence property of the qubit, because the spectral density of dilatational waves is higher than that of the flexural waves. As mentioned above, the decoherence time T_d is mainly determined by the contribution of the dilatational waves. From equations (15) and (18), this result directly affects the population and quality factor. On the contrary, the influence of the flexural waves prevails over that of the dilatational waves in the large Φ regime. For example, the ratios in spectral density of dilatational and flexural waves are about 6:1 and 1:354 for the cases of $\Phi = 0.05\pi$ and 0.45π, respectively.

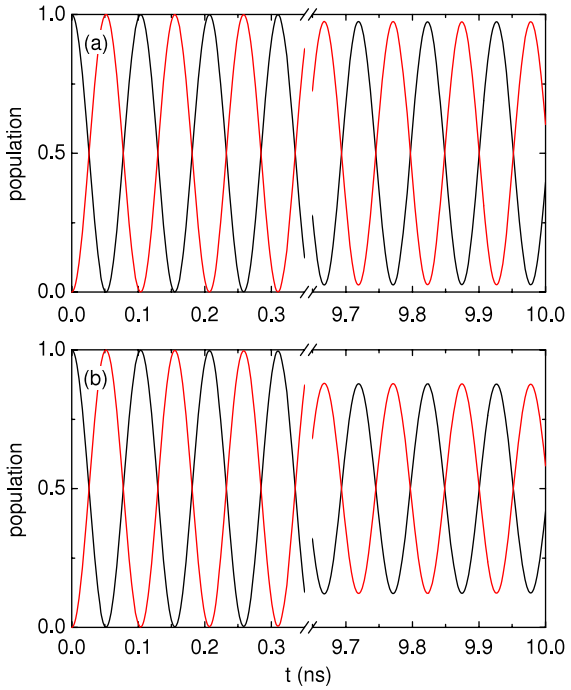

Figure 5. Time evolutions of the populations n_L (black line) and n_R (red line) for (a) $\Phi = 0.1\pi$ and (b) $\Phi = 0.4\pi$. The tunnel coupling is $T_c = 20$ μeV.

(This figure is in colour only in the electronic version)

Therefore, by varying the interdot orientation, the dominant contribution of the quality factor can be transferred between two waves.

Figure 5 further shows the dynamics of the qubit in the cases of different angles Φ. The value of T_c is fixed at 20 μeV. The amplitudes of the populations vary slightly in the short-time regime. For $\Phi = 0.1\pi$, the effect of the damping on the oscillation is observed in the long-time regime (figure 5(a)). As the angle increases, the damping becomes large and the amplitude of the population is clearly suppressed as shown in figure 5(b). We evaluate two systems. It is expected that the system with $\Phi = 0.4\pi$ loses coherence faster than the case with $\Phi = 0.1\pi$. To perform enough computational steps, the free-standing qubit with a small angle operates more effectively due to the longer decoherence time.

4. Conclusions

In this paper we have reported the decoherence of a free-standing qubit induced by confined phonons. The characteristic of the qubit is significantly modified by changing the tunnel coupling. We also investigated the effect of spatial arrangement of the dots on the quality of the system. The calculations showed that the evolution of the quantum states strongly depends on the interdot direction. With external control of the related parameters, we are able to better understand the underlying physics of the decoherence phenomenon and make a theoretical study of the performance of a double dot qubit based on a free-standing structure.

Acknowledgments

This work is supported by the National Science Council, Taiwan under grant numbers NSC 97-2112-M-390-006-MY3 and 98-2112-M-006-002-MY3.

References

[1] Komiyama S, Astafiev O, Antonov V, Kutsuwa T and Hiral H 2000 *Nature* **403** 405
[2] Chan I H, Westervelt R M, Maranowski K D and Gossard A C 2002 *Appl. Phys. Lett.* **80** 1818
[3] Zrenner A, Beham E, Stufler S, Findeis F, Bichler M and Abstreiter G 2002 *Nature* **418** 612
[4] Loss D and DiVicenzo D P 1998 *Phys. Rev.* A **57** 120
[5] Reimann S M and Manninen M 2002 *Rev. Mod. Phys.* **74** 1283
[6] van der Wiel W G, De Franceschi S, Elzerman J M, Fujisawa T, Tarucha S and Kouwenhoven L P 2003 *Rev. Mod. Phys.* **75** 1
[7] Hayashi T, Fujisawa T, Cheong H D, Jeong Y H and Hirayama Y 2003 *Phys. Rev. Lett.* **91** 226804
[8] Gorman J, Hasko D G and Williams D A 2005 *Phys. Rev. Lett.* **95** 090502
[9] Petta J R, Johnson A C, Marcus C M, Hanson M P and Gossard A C 2004 *Phys. Rev. Lett.* **93** 186802
[10] Brandes T and Vorrath T 2002 *Phys. Rev.* B **66** 075341
[11] Stavrou V N and Hu X 2005 *Phys. Rev.* B **72** 075362
[12] Ramirez H Y, Camacho A S and Lew Yan Voon L C 2007 *J. Phys.: Condens. Matter* **19** 346216
[13] Fedichkin L and Privman V 2009 *Electron Spin Resonance and Related Phenomena in Low-Dimensional Structures* ed M Fanciulli (Berlin: Springer)
[14] Fedichkin L and Fedorov A 2004 *Phys. Rev.* A **69** 032311
[15] Wu Z J, Zhu K D, Yuan X Z, Jiang Y W and Zheng H 2005 *Phys. Rev.* B **71** 205323
[16] Vorojtsov S, Mucciolo E R and Baranger H U 2005 *Phys. Rev.* B **71** 205322
[17] Thorwart M, Eckel J and Mucciolo E R 2005 *Phys. Rev.* B **72** 235320
[18] Hohenester U 2006 *Phys. Rev.* B **74** 161307(R)
[19] Storcz M J, Hartmann U, Kohler S and Wilhelm F K 2005 *Phys. Rev.* B **72** 235321
[20] Hentschel M, Valente D C B, Mucciolo E R and Baranger H U 2007 *Phys. Rev.* B **76** 235309
[21] Nishiguchi N, Ando Y and Wybourne M N 1997 *J. Phys.: Condens. Matter* **9** 5751
[22] Balandin A and Wang K L 1998 *J. Appl. Phys.* **84** 6149
[23] Krummheuer B, Axt V M and Kuhn T 2002 *Phys. Rev.* B **65** 195313
[24] Weig E M, Blick R H, Brandes T, Kirschbaum J, Wegscheider W, Bichler M and Kotthaus J P 2004 *Phys. Rev. Lett.* **92** 046804
[25] Lindwall G, Wacker A, Weber C and Knorr A 2007 *Phys. Rev. Lett.* **99** 087401
[26] Kirschbaum J, Höhberger E M, Blick R H, Wegscheider W and Bichler M 2002 *Appl. Phys. Lett.* **81** 280
[27] Rossler C, Bichler M, Schuh D, Wegscheider W and Ludwig S 2008 *Nanotechnology* **19** 165201
[28] Auld B A 1973 *Acoustic Fields and Waves in Solids* (New York: Wiley)
[29] Donetti L, Gámiz F, Roldán J B and Godoy A 2006 *J. Appl. Phys.* **100** 013701
[30] Bannov N, Aristov V, Mitin V and Stroscio M A 1995 *Phys. Rev.* B **51** 9930
[31] Debald S, Brandes T and Kramer B 2002 *Phys. Rev.* B **66** 041301(R)
[32] Liao Y Y, Chuu D S and Jian S R 2008 *J. Appl. Phys.* **104** 104315

[33] Leggett A J, Chakravarty S, Dorsey A T, Fisher M P A, Garg A and Zwerger W 1987 *Rev. Mod. Phys.* **59** 1
[34] Pollard W T and Friesner R A 1994 *J. Chem. Phys.* **100** 5054
[35] Weiss U 1999 *Quantum Dissipative Systems* (Singapore: World Scientific)
[36] Stavrou V N and Hu X 2006 *Phys. Rev.* B **73** 205313
[37] Bruus H, Flensberg K and Smith H 1993 *Phys. Rev.* B **48** 11144
[38] Glavin B A, Pipa V I, Mitin V V and Stroscio M A 2002 *Phys. Rev.* B **65** 205315